Available online at www.sciencedirect.com
ScienceDirect
International Journal of Mass Spectrometry 261 (2007) 32–37
International Journal of Mass Spectrometry
www.elsevier.com/locate/ijms

Ionization-induced proton transfer in thymine–ammonia van der Waals clusters

Nam Joon Kim [a,*], Hyung Min Kim [b], Seong Keun Kim [b,*]

[a] *Department of Chemistry, Chungbuk National University, Chungbuk 361-763, Republic of Korea*
[b] *School of Chemistry, Seoul National University, Seoul 151-747, Republic of Korea*

Received 15 June 2006; received in revised form 24 July 2006; accepted 24 July 2006
Available online 24 August 2006

Abstract

Ion intensity distribution of thymine–ammonia clusters produced in a supersonic jet was investigated using the resonant 2-photon ionization technique. The mass spectrum of $Thy_m(NH_3)_n$ ($m = 1$–7) exhibited an anomalously strong ion intensity for $n = 1$ in contrast to the nearly negligible ion signals for $n > 1$. We suggest that proton transfer from the thymine radical cation to an ammonia molecule following the ionization of the clusters is responsible for the observed anomaly. It is also proposed that charge migration occurring with the proton transfer leads to an ion core switch from the thymine radical cation to the newly formed ammonium ion. The subsequent evaporation of other ammonia molecules in the cluster ion as a consequence of the energy released from the reaction results in extensive loss of ion signals for $n > 1$, and at their expense, an anomalously large ion intensity for $n = 1$. This mechanism is supported by density functional theory calculations on the thymine–ammonia 1:1 complex ion performed along the reaction coordinate of the proton transfer. The formation of the ammonium ion in the cluster is also confirmed by the fragmentation feature of metastable $Thy_m(NH_3)_1^+$ ($m = 1$–4) obtained using reflectron time-of-flight mass spectrometry.

Keywords: Proton transfer; Thymine; van der Waals cluster; Resonant 2-photon ionization; Reflectron time-of-flight mass spectrometry

1. Introduction

Ionizing radiation causes mutagenic and carcinogenic effects in a mammalian cell [1–3]. It is widely accepted that DNA is the primary target for the radiation-induced lethality [3–5]. In particular, double-strand breaks, which are one of the most critical cytotoxic DNA lesions [3], are directly initiated by ionizing radiation that generates DNA base radical cations [6]. With the decreased basicity of DNA bases in their ionic state, the radical cation gains considerable acidity [7] and undergoes proton transfer to its complementary base in a DNA base pair, which leads to the breakage in a DNA double-strand [8].

Many studies have been performed on the radical cations of DNA bases and their reactions in solution, in the solid state, and even in the gas phase [6,8–11]. Much attention has been paid to guanine and adenine radical cations in view of their roles in charge transport in DNA [12]. By comparison, the reactions of the thymine radical cation that has the highest oxidation potential among the four DNA bases [13,14] have been scarcely studied.

The high oxidation potential of thymine implies difficulty of forming a thymine radical cation in DNA, but also indicates that thymine radical cation is more prone to react with other species, once it is formed. It was proposed that the greater stability of the radical cations of purines than of pyrimidines could give the former a longer lifetime so that they could be more easily repaired by recombination processes. It is to be noted that in quinine sensitized photo-oxidation of purines and pyrimidines, only the pyrimidine radical cations generated photo-products [15]. In this regard, the reactions of the thymine radical cation can be critical in the DNA photo-damage caused by ionizing radiation that initially generates randomly distributed radical cations of DNA bases.

Since Sevilla [16,17] first showed that UV irradiation of thymine at 77 K in both alkaline and acidic glasses can produce the thymine radical cations, their reactions have been extensively studied in the past decades [7,15,17,18]. Electron spin resonance (ESR) and electron paramagnetic resonance/electron nuclear

* Corresponding authors.
E-mail addresses: namjkim@chungbuk.ac.kr (N.J. Kim), seongkim@snu.ac.kr (S.K. Kim).

1387-3806/$ – see front matter © 2006 Elsevier B.V. All rights reserved.
doi:10.1016/j.ijms.2006.07.017

double resonance (EPR/ENDO) have been applied to identify the reaction products of the thymine radical cation in the condensed phase [19]. The formation and decay of the thymine radical cations in solution were directly monitored in nanosecond time scale by transient absorption [20] and time-resolved FT-EPR [21]. Theoretical calculations on radiation-induced damage of thymine derivatives were also intensively carried out [22–24]. Despite all these studies, the reactions of the thymine radical cation have never been observed in the gas phase to our knowledge.

Molecular clusters produced in a supersonic jet provide an ideal system to study ion–molecule reactions at the molecular level [25–28]. The cluster ion distribution with anomalously strong ion peaks for certain cluster sizes has often been used to deduce the mechanism of ion–molecule reactions in the cluster [27,28]. Here, we investigated ion intensity distribution of thymine–ammonia clusters using the resonant 2-photon ionization (R2PI) technique. An anomalous ion intensity distribution was observed in the mass spectrum, which was explained by the transfer of a proton from the thymine radical cation to an ammonia molecule in the cluster ion followed by extensive thermal evaporation of other ammonia molecules with the excess energy of the reaction. Density functional theory (DFT) calculations on the thymine–ammonia 1:1 complex ion were performed to support the proposed mechanism. The fragmentation process of metastable $Thy_m(NH_3)_1^+$ ($m = 1$–4) was also investigated using reflectron time-of-flight mass spectrometry to further confirm the mechanism of the proton transfer forming the ammonium ion in the cluster.

2. Experimental methods

The experimental set-up was described elsewhere [29]. Briefly, the apparatus is a typical molecular beam machine with a linear time-of-flight mass spectrometer (TOF-MS). The powder sample of thymine was heated to 230 °C in a metal oven, and the vapor was expanded through a 0.5-mm hole of a pulsed nozzle with a mixture of ammonia and argon at a total stagnation pressure of 1–2 atm. The expanded gas passed through a 1-mm hole of a skimmer and was ionized by R2PI using ns or fs laser pulses in the ionization region of TOF-MS. The ions were accelerated toward a field-free region of TOF-MS and then detected by a microchannel plate.

The fourth harmonic of an Nd:YAG laser (266 nm, 6 ns, 10 mJ/pulse) was used in ns-R2PI. For fs-R2PI, the third harmonic (267 nm, 400 fs, 1 μJ/pulse) of the fundamental light generated by a commercial regeneratively amplified Ti:sapphire laser was used. Thymine was purchased from Aldrich Chemical Company and used without further purification.

3. Results and discussion

Fig. 1a and b shows the mass spectra of $Thy_m(NH_3)_n$ ($m = 1$–7) obtained by ns- and fs-R2PI, respectively. The previously reported even–odd alternation in the ion intensities of unsolvated thymine clusters is clearly seen in Fig. 1a but not in Fig. 1b, as reported and explained in earlier papers [30,31].

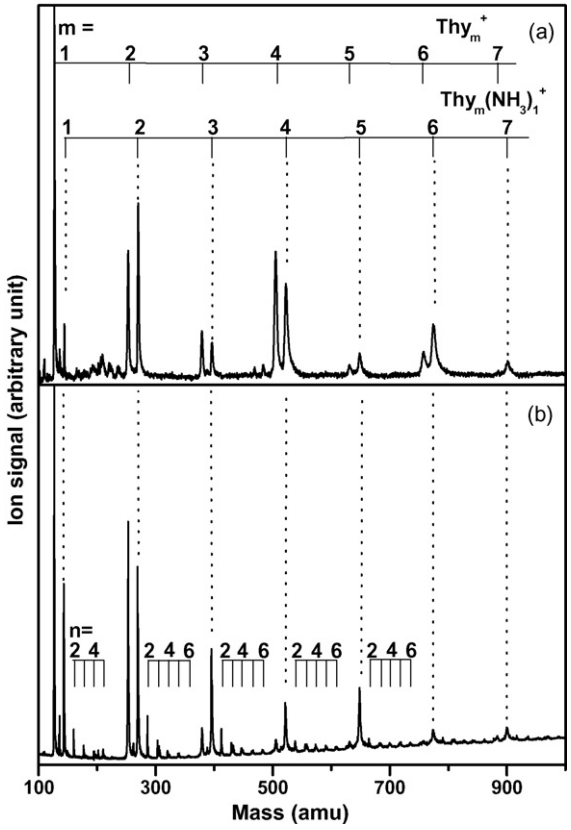

Fig. 1. Mass spectra of $Thy_m(NH_3)_n^+$ obtained by R2PI using (a) ns and (b) fs laser pulses. The dotted lines indicate ion signals of $Thy_m(NH_3)_1^+$. The ion signals for $n > 1$ in (b) are denoted by the number n.

The most interesting feature observed in both mass spectra is that the ion intensity for $n = 1$ of $Thy_m(NH_3)_n^+$ is anomalously strong compared with those for $n > 1$. In Fig. 1a the ion signals for $n > 1$ are completely absent, and in Fig. 1b they are less than one fifth of the ion signal for $n = 1$. This is quite a unique feature that has never been observed in the mass spectra of solvated van der Waals clusters. Even the R2PI mass spectra of the closely related species $Ade_m(NH_3)_n$ [32] and $Thy_m(H_2O)_n$ [33] did not exhibit this feature. Only the unique combination of Thy and NH_3 seems to yield such anomaly.

It is possible that the anomalous feature may simply represent the abundance of neutral clusters produced in the supersonic jet. In other words, the strong ion signal for $n = 1$ may indicate the extra stability of the mono-ammoniated thymine clusters over other ammoniated thymine clusters, possibly due to stronger binding of the first ammonia molecule to thymine than the subsequent binding. This scenario is not likely, however, because the anomalous feature is observed for all sizes of thymine clusters ($m = 1$–7), the majority of which have more than one first-binding sites for ammonia molecules.

Although it is possible in principle that the anomalous feature is due to different ionization cross-sections of the clusters, it is rather unlikely for the following reasons: First, the chromophores of $Thy_m(NH_3)_1$ and $Thy_m(NH_3)_n$ ($n > 1$) in R2PI at 266 nm are same. Second, the R2PI spectrum of thymine in a supersonic jet exhibits only broad and unstructured absorption

starting at around 277 nm [34]. Hence, it is unlikely that the electronic absorption spectrum of $Thy_m(NH_3)_1$ shows any sharp resonance band near 266 nm, which is absent in the spectrum of $Thy_m(NH_3)_n$ ($n > 1$). Third, the 2-photon energy of 266 nm (9.3 eV) is higher than the ionization potential (IP) of thymine (8.9 eV) [13] and therefore, well above those of $Thy_m(NH_3)_n$ [35]. For this reason, an abrupt change in the ionization efficiency with the number of solvent molecules n will not occur in the R2PI of $Thy_m(NH_3)_n$ at 266 nm. This is further supported by the fact that the R2PI mass spectrum of $Thy_m(H_2O)_n$ does not exhibit the anomalous feature.

Since the anomalous feature in the mass spectrum of $Thy_m(NH_3)_n^+$ does not result from the intrinsic stability or different ionization cross-sections of neutral clusters, it is likely due to some reactions that occur in the cluster during the ionization process. In R2PI, a molecule is ionized by absorbing two photons simultaneously or sequentially within the temporal width of the laser pulse. The first photon excites the molecule to one of the electronic excited states and the second photon ionizes the excited molecule. Hence, the reaction responsible for any anomalous distribution in the mass spectrum may occur either in the electronic excited state or in the ionic state.

Between these two possibilities, we ruled out the reaction occurring in the excited state because the anomalous ion intensity distribution was observed in both Fig. 1a and b, regardless of the laser pulse width. Since the progress of a reaction in the electronic excited state during R2PI is limited by the temporal width of the laser pulse, the mass spectral feature resulting from the reaction should be markedly different between ns-R2PI and fs-R2PI, unless the reaction is so fast to be complete within the pulse width of the latter (~400 fs), which is very rare. We note that the hydrogen transfer in the excited state of phenol–$(NH_3)_{n=1-3}$ and the excited state proton transfer in naphthol–$(NH_3)_n$ clusters, both of which are among the fastest reactions, were reported to occur in a few tens of ps [36,37].

If, on the other hand, the reaction time in the electronic excited state is longer than the laser pulse width, the excited molecules will be mostly ionized before the reaction takes place and the mass spectral feature will not be affected by the reaction.

As a contrasting case, it is worth noting that the even-odd alternation in the ion intensity distribution of unsolvated thymine clusters, which is due to intracluster photo-dimerization in the electronic excited state [30], is not observed in the fs-R2PI mass spectrum (Fig. 1b), but clearly seen in the ns-R2PI mass spectrum (Fig. 1a). Therefore, the observed anomaly for $Thy_m(NH_3)_1^+$ in both the ns- and fs-R2PI mass spectra indicates that it results from a reaction not in the electronic excited state but in the ionic state of the cluster.

We should therefore now focus our attention to what kind of reaction in the ionic state causes the loss of ion signals of $Thy_m(NH_3)_n^+$ for $n > 1$ in contrast to the strong ion intensity for $n = 1$. We suggest that a most likely candidate should be the proton transfer from the thymine radical cation to an ammonia molecule in the cluster following the ionization. This is supported by the fact that thymine obtains considerable acidity upon ionization by becoming the thymine radical cation [7]. Beckert and co-workers [21] also suggested that deprotonation in the

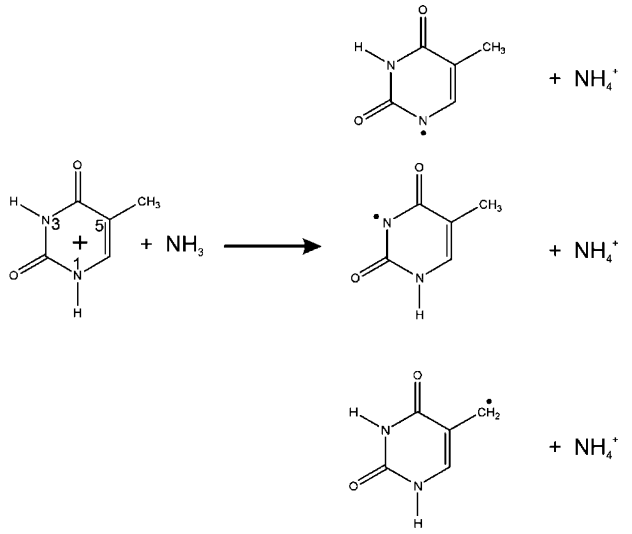

Scheme 1.

N1 site is a dominant reaction channel of pyrimidine radical cations in aqueous solution (Scheme 1). The deprotonated radical at >C5–CH_3 was identified as a major product of ionizing radiation for thymine in aqueous glasses at 77 K or anhydrous thymine crystals [16,19,38].

To find out if the proton transfer can occur in the thymine–ammonia van der Waals clusters as in the condensed phase, we performed DFT calculations on the thymine–ammonia 1:1 complex ion using the GAUSSIAN 03 package [39]. The structures were fully optimized with DFT employing a hybrid functional of UB3LYP with a standard 6-31+G(d,p) basis set. The optimized structures are shown in Fig. 2.

Three hydrogen-bonded forms were found and labeled as $HB1^+$, $HB2^+$, and $HB3^+$. The fully optimized structure of $HB1^+$ could not be obtained due to its convergence to the proton-transferred form ($PT1^+$) during the optimization process. The $HB1^+$ in Fig. 2 is thus a partially optimized structure with a fixed bond length of N1–H at 1.12 Å. The relative energies for the hydrogen-bonded and proton-transferred forms without zero-point energy correction are shown in Fig. 3. The relaxed potential energy surface scan as a function of the N (1 or 3)–H or C–H distance was also performed at the UB3LYP/6-31G(d) level to find any reaction barrier for the proton transfer. Interestingly, no barrier was found for the proton transfer of $HB1^+$ and $HB3^+$. Only $HB2^+$ was predicted to have a barrier. With optimization of the transition state ($TS2^+$) at the UB3LYP/6-31+G(d,p) level, the barrier height was estimated to be 0.77 kcal/mol.

These results of calculations are quite consistent with the observations in the earlier condensed phase study [16,19,21,38], which found the deprotonation at N1–H or >C5–CH_3 was the main reaction channel for the thymine radical cation. Therefore, we conclude that the proton transfer of the thymine radical cation can occur in the thymine–ammonia clusters.

The proposed mechanism is illustrated in Fig. 4. The R2PI of $Thy_m(NH_3)_n$ generates a thymine radical cation within the cluster. A proton of the thymine radical cation is then transferred to an ammonia molecule, resulting in the ion core switch within

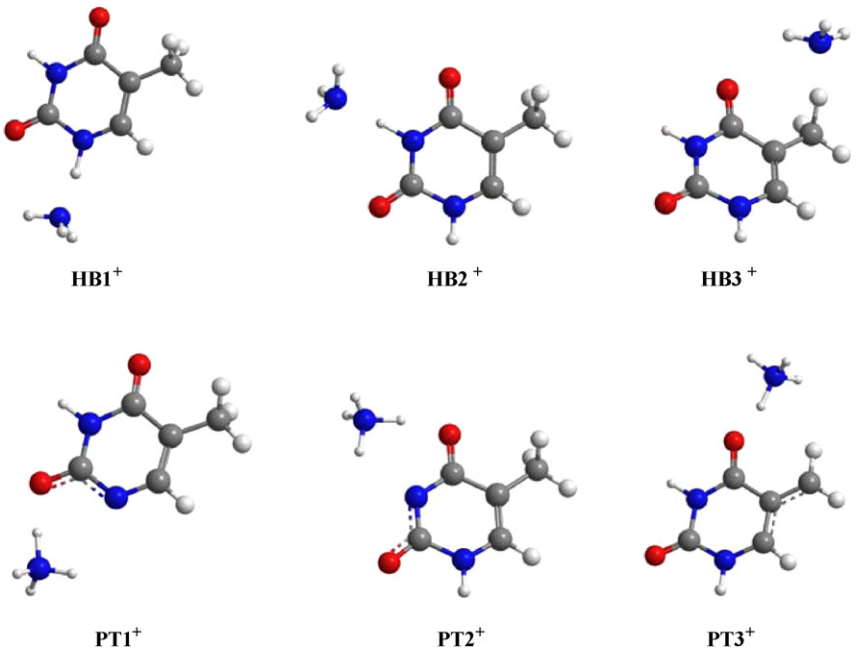

Fig. 2. The optimized structures of $Thy_1(NH_3)_1^+$ calculated at the UB3LYP/6-31+G(d,p) level. The hydrogen-bonded cluster ions are labeled as $HB1^+$, $HB2^+$, and $HB3^+$ and the corresponding products of proton transfer as $PT1^+$, $PT2^+$, and $PT3^+$. The fully optimized structure of $HB1^+$ could not be obtained due to its convergence to $PT1^+$ during the optimization. Therefore, $HB1^+$ is the structure obtained by partial optimization with a fixed bond length of N1–H (see the text).

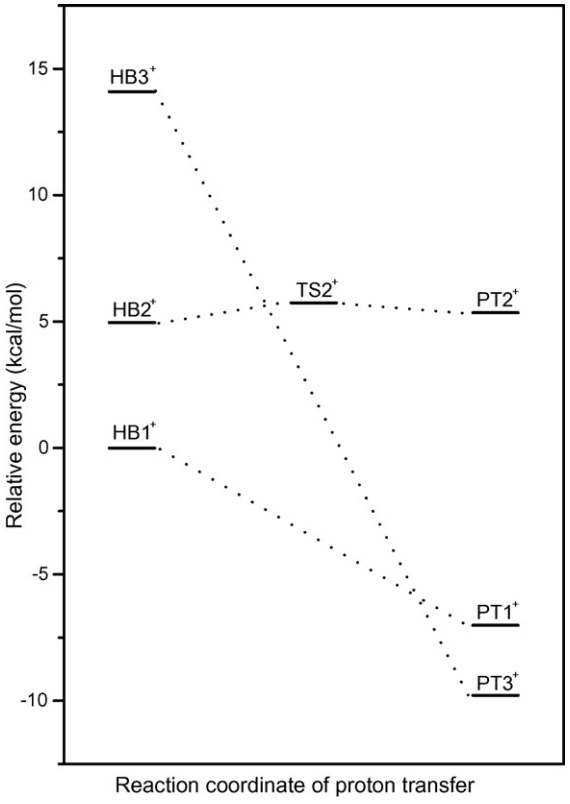

Fig. 3. Energy level diagram showing the relative energies of the reactants ($HB1^+$, $HB2^+$, $HB3^+$), the transition state ($TS2^+$), and the products ($PT1^+$, $PT2^+$, $PT3^+$) along the reaction coordinate for proton transfer. Energy values were calculated at the UB3LYP/6-31+G(d,p) level without zero-point energy correction. The energy of $HB1^+$ is the single-point energy at the partially optimized structure (see the text).

the cluster from the thymine radical cation to the newly formed ammonium ion. The final step is evaporation of most neutral solvents by the energy released from the reaction. This leads to the loss of ion signals for $n > 1$ of $Thy_m(NH_3)_n^+$, while increasing the ion signal for $n = 1$.

To verify the formation of ammonium ion in the cluster through proton transfer, we investigated metastable fragmentation of $Thy_m(NH_3)_1^+$ using a reflectron TOF-MS. When a metastable cluster ion decomposes into a daughter ion and a neutral fragment in the field-free region of the TOF-MS, the daughter ion carries a kinetic energy of $E_d = (M_d/M_p)E_p$, where M_d and M_p are the masses of the daughter and parent ions, respectively, and E_p is the parent ion energy. Because of the difference in the kinetic energy, the daughter and the parent ions penetrate into the reflectron by different amounts to obtain different flight times, and thus become separately detected.

Fig. 5a shows the mass spectrum near the mass of $Thy_1(NH_3)_1^+$ obtained by a refelctron TOF-MS under basically the same experimental conditions as used for Fig. 1. The mass spectra of Fig. 5b and c show the daughter ion signals that come from dissociation of parent $Thy_1(NH_3)_1^+$, which were obtained by applying a lower voltage (U_r^d) to the reflectron than that used in Fig. 5a (U_r^p). By setting $U_r^d = (M_d/M_p)U_r^p$, we can make the daughter ion follow the same path in the reflectron with the parent ion and arrive at the detector in the same flight time [40]. The ion signal of the daughter ions was fitted to a Gaussian function and then integrated to obtain their ion intensities.

The most remarkable finding is that NH_4^+ is produced by fragmentation of $Thy_1(NH_3)_1^+$ (Fig. 5c), which suggests that the parent ion $Thy_1(NH_3)_1^+$ contains an NH_4^+ ion core and a $(Thy–H)^\bullet$ radical, in a distinctly different composition from that of a Thy^+ core and NH_3. This result strongly supports our mecha-

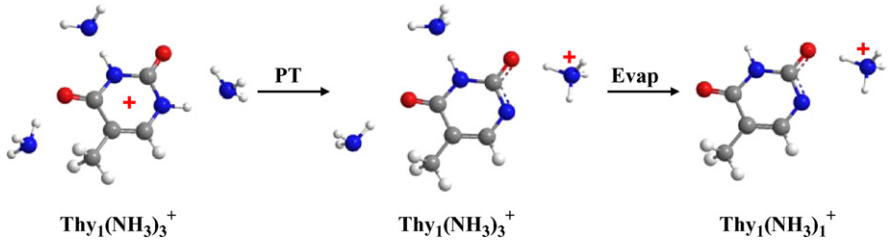

Fig. 4. Schematic diagram for the proton transfer in $Thy_m(NH_3)_n^+$ that leads to a strong ion signal for $Thy_m(NH_3)_1^+$ and simultaneous reduction in the ion signals of $Thy_m(NH_3)_n^+$ for $n>1$. An initial system of $Thy_1(NH_3)_3^+$ was chosen for an illustrative example. PT and Evap represent proton transfer and evaporation of the solvents, respectively.

nism for ammonium ion formation through proton transfer from thymine radical cation to ammonia following the ionization of $Thy_1(NH_3)_n$.

We note, however, that fragmentation also yields the molecular ion Thy^+ in addition to NH_4^+ (Fig. 5b), which indicates that some of the parent ions may exist in the form of a complex between Thy^+ and NH_3. From the relative daughter ion intensity of NH_4^+ to Thy^+, it is estimated that at least 16% of the parent ions have NH_4^+ as the core ion.

It is interesting to note that this percentage increases as the cluster size becomes larger. In order to better represent the fragmentation propensity, we define the fragmentation ratio γ as $\gamma_i = I_i/(I_A + I_{T-H} + I_T)$ with i = A or T–H or T, where I_A, I_{T-H}, and I_T are the intensities of the daughter ions from the loss of NH_3, the $(Thy–H)^\bullet$ radical, and the Thy neutral molecule, respectively. Fig. 6 shows γ_i measured for parent ions of $Thy_m(NH_3)_1^+$ (m = 1–4). For m = 1 and 2, the loss of NH_3 occurs more extensively than that of Thy or $(Thy–H)^\bullet$, which implies that a large fraction of the parent ions have Thy^+ as the core ion. For m = 3 and 4, however, the loss of $(Thy–H)^\bullet$ becomes totally predominant, with more than 80% of the fragmentation occurring via the $(Thy–H)^\bullet$ loss in contrast to the NH_3 loss channel that accounts for less than 4%. These results clearly show that NH_4^+ rapidly becomes the core ion as the cluster size increases in $Thy_m(NH_3)_1^+$.

The fact that such an anomalous distribution is not observed when the solvents are water, *i.e.*, for $Thy_m(H_2O)_n^+$, can be explained by the low proton affinity of H_2O [41]. The proton affinity of H_2O is about 40 kcal/mol less than that of NH_3, which would render the proton transfer reaction considerably more endothermic.

In summary, an anomalous ion intensity distribution was observed in the R2PI mass spectrum of $Thy_m(NH_3)_n^+$, with a strong ion intensity for n = 1 and negligible ion signals for $n>1$. The culprit was proposed to be the proton transfer from the thymine radical cation to an ammonia molecule in the cluster following the ionization, which also causes the ion core switch from the thymine radical cation to the ammonium ion. Subsequent evaporation of neutral ammonia solvents results in extensive loss of ion signals for $Thy_m(NH_3)_n^+$ ($n>1$), while increasing the ion signal for $Thy_m(NH_3)_1^+$ where NH_4^+ is now the ion core.

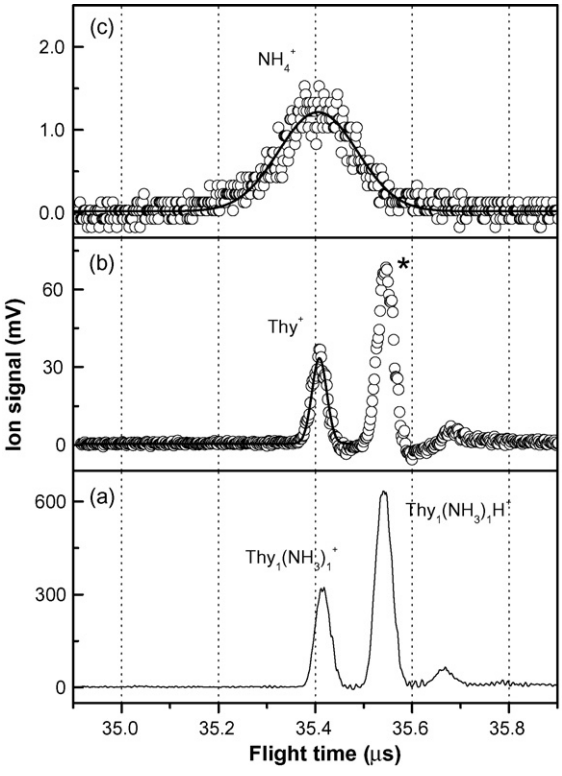

Fig. 5. (a) Reflectron TOF mass spectra of $Thy_m(NH_3)_n$ in the vicinity of the flight time for $m=n=1$, obtained by R2PI with ns laser pulses at 266 nm. (b) and (c) are the same mass spectra showing respectively the daughter ions of the NH_3 and $(Thy–H)^\bullet$ loss channel from the parent ion of $Thy_1(NH_3)_1^+$. The applied voltages at the reflectron were (a) +2800 V, (b) +2467 V, and (c) +352 V. The ion signals (◯) were fitted to a Gaussian function (solid line). Asterisk (*) represents the ion peak resulting from the loss of NH_3 from $Thy_1(NH_3)_1H^+$.

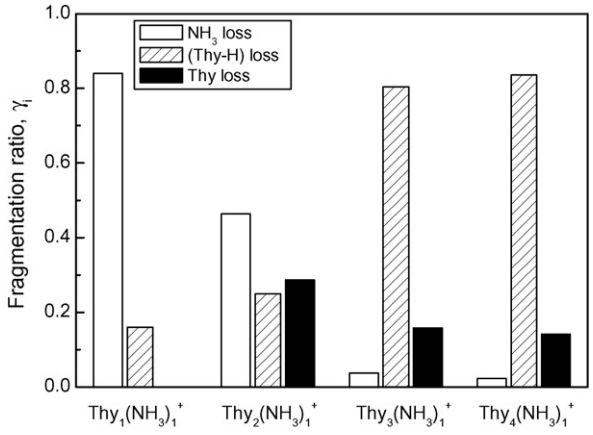

Fig. 6. Plot of the fragmentation ratio, γ_i, for $Thy_m(NH_3)_1^+$ (m = 1–4).

The present study shows that a process such as proton transfer can become a facile photo-induced reaction channel in solvated nucleobase when the solvent has a large proton affinity.

Acknowledgements

This work was supported by Chungbuk National University Grant in 2004 to NJK and the Star Faculty Program of the Korea Research Foundation to SKK.

References

[1] C. von Sonntag, The Chemical Basis of Radiation Biology, Taylor and Francis, London, 1987.
[2] M. Yan, D. Becker, S. Summerfield, P. Renke, M.D. Sevilla, J. Phys. Chem. 96 (1992) 1983.
[3] J.B. Little, Carcinogenesis 21 (2000) 397.
[4] F. Urbach, The Biological Effects of Ultraviolet Radiation, Pergamon, New York, 1969.
[5] G.J. Kantor, Photochem. Photobiol. 41 (1985) 741.
[6] C.T. Hwang, C.L. Stumpf, Y.-Q. Yu, H.I. Kenttämaa, Int. J. Mass Spectrom. 182/183 (1999) 253.
[7] S. Steenken, Free Radic. Res. Commun. 16 (1992) 349.
[8] S. Steenken, Chem. Rev. 89 (1989) 503.
[9] D.M. Close, J. Phys. Chem. B 107 (2003) 864.
[10] K. Kobayashi, S. Tagawa, J. Am. Chem. Soc. 125 (2003) 10213.
[11] J.M. Price, C.J. Petzold, H.C.M. Byrd, H.I. Kenttämaa, Int. J. Mass Spectrom. 212 (2001) 455.
[12] T. Takada, K. Kawai, M. Fujitsuka, T. Majima, Proc. Natl. Acad. Sci. U.S.A. 101 (2004) 14002.
[13] K.-W. Choi, J.-H. Lee, S.K. Kim, J. Am. Chem. Soc. 127 (2005) 15674.
[14] C.E. Crespo-Hernández, R. Arce, Y. Ishikawa, L. Gorb, J. Leszczynski, D.M. Close, J. Phys. Chem. A 108 (2004) 6373.
[15] J.R. Wagner, J.E. van Lier, L.J. Johnston, Photochem. Photobiol. 52 (1990) 333.
[16] M.D. Sevilla, J. Phys. Chem. 75 (1971) 626.
[17] M.D. Sevilla, C.V. Paemel, G. Zorman, J. Phys. Chem. 76 (1972) 3577.
[18] D.J. Deeble, M.N. Schuchmann, S. Steenken, C. von Sonntag, J. Phys. Chem. 94 (1990) 8186.
[19] D.M. Close, Radiat. Res. 135 (1993) 1.
[20] R. Lomoth, O. Brede, Chem. Phys. Lett. 288 (1998) 47.
[21] J. Geimer, O. Brede, D. Beckert, Chem. Phys. Lett. 276 (1997) 411.
[22] D. Close, G. Forde, L. Gorb, J. Leszczynski, Struct. Chem. 14 (2003) 451.
[23] S.D. Wetmore, F. Himo, R.J. Boyd, L.A. Eriksson, J. Phys. Chem. B 102 (1998) 7484.
[24] S. Naumov, A. Barthel, J. Reinhold, F. Dietz, J. Geimer, D. Beckert, Phys. Chem. Chem. Phys. 2 (2000) 4207.
[25] B. Brutschy, Chem. Rev. 92 (1992) 1567.
[26] A.W. Castleman Jr., S. Wei, Annu. Rev. Phys. Chem. 45 (1994) 685.
[27] M.T. Coolbaugh, G. Vaidyanathan, W.R. Peifer, J.F. Garvey, J. Phys. Chem. 95 (1991) 8337.
[28] G.M. Daly, M.S. El-Shall, J. Phys. Chem. 99 (1995) 5283.
[29] H. Kang, K.T. Lee, S.K. Kim, Chem. Phys. Lett. 359 (2002) 213.
[30] N.J. Kim, H. Kang, G. Jeong, Y.S. Kim, K.T. Lee, S.K. Kim, Proc. Natl. Acad. Sci. U.S.A. 98 (2001) 4841.
[31] N.J. Kim, H. Kang, G. Jeong, Y.S. Kim, K.T. Lee, S.K. Kim, J. Chem. Phys. 115 (2001) 7002.
[32] N.J. Kim, H. Kang, G. Jeong, Y.S. Kim, K.T. Lee, S.K. Kim, J. Phys. Chem. A 104 (2000) 6552.
[33] N.J. Kim, Y.S. Kim, G. Jeong, T.K. Ahn, S.K. Kim, Int. J. Mass Spectrom. 219 (2002) 11.
[34] B.B. Brady, L.A. Peteanu, D.H. Levy, Chem. Phys. Lett. 147 (1988) 538.
[35] S.K. Kim, W. Lee, D.R. Herschbach, J. Phys. Chem. 100 (1996) 7933.
[36] G. Grégoire, C. Dedonder-Lardeux, C. Jouvet, S. Martrenchard, A. Peremans, D. Solgadi, J. Phys. Chem. A 104 (2000) 9087.
[37] R. Knochenmuss, I. Fischer, Int. J. Mass Spectrom. 220 (2002) 343.
[38] W.A. Bernhard, J. Barnes, K.R. Mercer, N. Mroczka, Radiat. Res. 140 (1994) 199.
[39] M.J. Frisch, G.W. Trucks, H.B. Schlegel, G.E. Scuseria, M.A. Robb, J.R. Cheeseman, J.A. Montgomery Jr., T. Vreven, K.N. Kudin, J.C. Burant, J.M. Millam, S.S. Iyengar, J. Tomasi, V. Barone, B. Mennucci, M. Cossi, G. Scalmani, N. Rega, G.A. Petersson, H. Nakatsuji, M. Hada, M. Ehara, K. Toyota, R. Fukuda, J. Hasegawa, M. Ishida, T. Nakajima, Y. Honda, O. Kitao, H. Nakai, M. Klene, X. Li, J.E. Knox, H.P. Hratchian, J.B. Cross, C. Adamo, J. Jaramillo, R. Gomperts, R.E. Stratmann, O. Yazyev, A.J. Austin, R. Cammi, C. Pomelli, J.W. Ochterski, P.Y. Ayala, K. Morokuma, G.A. Voth, P. Salvador, J.J. Dannenberg, V.G. Zakrzewski, S. Dapprich, A.D. Daniels, M.C. Strain, O. Farkas, D.K. Malick, A.D. Rabuck, K. Raghavachari, J.B. Foresman, J.V. Ortiz, Q. Cui, A.G. Baboul, S. Clifford, J. Cioslowski, B.B. Stefanov, G. Liu, A. Liashenko, P. Piskorz, I. Komaromi, R.L. Martin, D.J. Fox, T. Keith, M.A. Al-Laham, C.Y. Peng, A. Nanayakkara, M. Challacombe, P.M.W. Gill, B. Johnson, W. Chen, M.W. Wong, C. Gonzalez, J.A. Pople, Gaussian 03, Revision C.02, Gaussian Inc., Wallingford, CT, 2004.
[40] S. Wei, W.B. Tzeng, A.W. Castleman Jr., J. Chem. Phys. 92 (1990) 332.
[41] S.G. Lias, J.F. Liebman, R.D. Levin, J. Phys. Chem. Ref. Data 13 (1984) 695.